Pergamon
www.elsevier.nl/locate/asr

Adv. Space Res. Vol. 23, No. 4, pp. 631–653, 1999
© 1999 COSPAR. Published by Elsevier Science Ltd. All rights reserved
Printed in Great Britain
0273-1177/99 $20.00 + 0.00

PII: S0273–1177(99)00160-X

THE INTERNATIONAL GPS SERVICE (IGS): AN INTERDISCIPLINARY SERVICE IN SUPPORT OF EARTH SCIENCES

G. Beutler[1], M. Rothacher[1], S. Schaer[1], T.A. Springer[1], J. Kouba[2], R.E. Neilan[3]

[1] *Astronomical Institute, University of Bern, Sidlerstrasse 5, CH-3012 Bern, Switzerland*
[2] *Geodetic Survey of Canada, Natural Resources Canada, 615 Booth Street, Ontario K1A0E9, Canada*
[3] *IGS Central Bureau, Jet Propulsion Laboratory, 4800 Oak Grove Drive, Pasadena, California 91109, USA*

ABSTRACT

Since 21 June 1992 the International GPS Service (IGS) produces and makes available uninterrupted time series of its products, in particular GPS observations from the IGS Global Network, GPS orbits, Earth orientation parameters (components x and y of polar motion, length of day), satellite and receiver clock information, and station coordinates and velocities.

At a later stage the IGS started exploiting its network for atmosphere monitoring, in particular for ionosphere mapping and for troposphere monitoring. This is why new IGS products encompass ionosphere maps and tropospheric zenith delays, both with a very high temporal resolution. This development will be even more pronounced through the advent of many space-missions carrying GPS, or combined GPS/GLONASS receivers for various purposes. The achievements of the IGS are only possible through a unique voluntary cooperation of a great number of active organizations.

This article gives an informative overview for the broader scientific community of the spectrum of problems that is addressed today using IGS/GPS techniques. ©1999 COSPAR. Published by Elsevier Science Ltd.

THE GLOBAL POSITIONING SYSTEM (GPS) AND ITS USE FOR SCIENCE

Since early 1994 the U.S. Global Positioning System (GPS) is fully operational. The constellation consists of 21 satellites (see Fig. 1) and three so-called active spares. The actual number of available satellites varies. In summer 1998 27 satellites are orbiting the Earth in six orbital planes, which are inclined by 55^o with respect to the equatorial plane and separated by 60^o on the equator. The orbital planes, as seen from the pole(s) and from a latitude of 35^o, are sketched in Fig. 2 (left, middle).

The "heart" of each GPS spacecraft is a high quality oscillator which is used to generate two coherent carriers $L1$ and $L2$ in the L-band (frequencies 1.57542 GHz and 1.22760 GHz) with wavelengths $\lambda_1 \approx 19$ cm and $\lambda_2 \approx 24$ cm. Information is transmitted using the phase modulation technique. The information consists of so-called C/A-code on $L1$, the precise P-code, or its encrypted version, the Y-code, on $L1$ and $L2$, and the broadcast information on $L1$, enabling the user of the system to compute the approximate broadcast satellite position at transmission time of a signal in the GPS time frame.

The GPS signals are recorded by GPS receivers. The "heart" of each receiver is its oscillator, which drives the receiver clock. Technical details concerning the actual generation of the code observations may be found, e.g., in Spilker (1980). The C/A-code is available to all users of the GPS, the P- resp. Y-code is reserved for military use. The C/A-code has a precision of about 3 meters (rms), the P- and Y-codes are about a factor of 10 more precise.

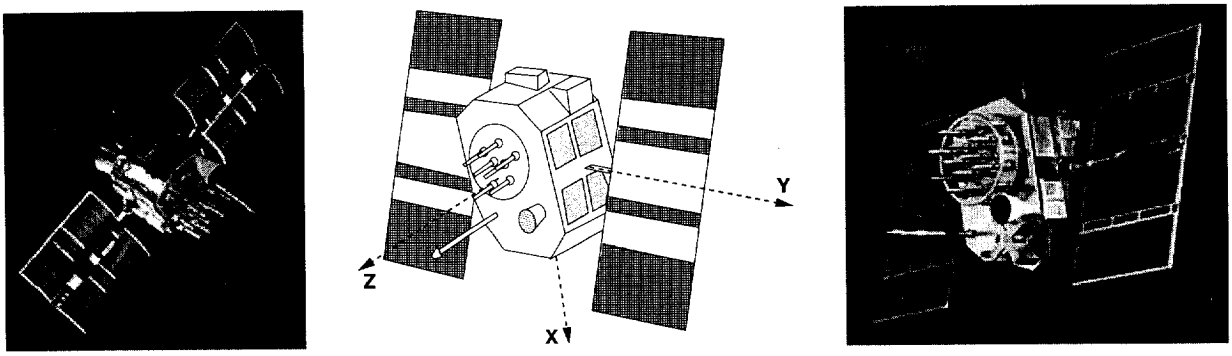

Fig. 1. GPS Block I Satellite; Schematic Figure; Block II Satellite

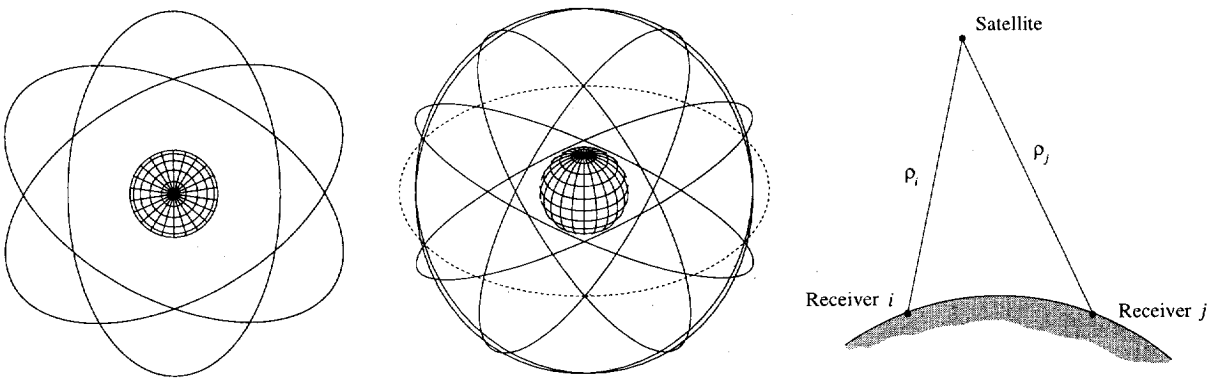

Fig. 2. The GPS Satellite System from a Latitude of 90^o and 35^o; Observing a Satellite j by the GPS Receivers i and k

The third picture in Fig. 2 illustrates the situation of a single observation for two receivers, i and k.

The C/A- and/or the P- or Y-code, as registered by receiver i at time t_i from satellite j, is defined as follows:

$$p_i^j = c \cdot (t_i - \tau^j)$$

where

t_i is the arrival time, or observation time, of a signal as measured by the clock of receiver i.

τ^j is the transmission time of the same signal, measured in the time frame of satellite j.

The pseudorange p_i^j may be related to the slant range ρ_i^j (Fig. 2) at time t_i and to the delays due to the Earth's atmosphere. The slant range is the geometrical distance between receiver at observation time t_i and the position of the satellite at time "τ^j":

$$p_i^j = \rho_i^j - c \cdot \Delta t^j + c \cdot \Delta t_i + \Delta\rho_{i,ion}^j + \Delta\rho_{i,trop}^j \tag{1}$$

where

c is the speed of light,

$\rho_i^j \doteq |\vec{r}(\tau^j) - \vec{R}(t_i)|$, $\vec{r}(\tau^j)$ being the satellite position at transmission time, $\vec{R}(t_i)$ being the position of receiver i at time t_i,

Δt^j is the error of the satellite clock w.r.t. a theoretical GPS-time,

Δt_i is the error of the receiver clock w.r.t. GPS-time.

$\Delta\rho_{i,trop}^j$ is the delay of the signal due to the neutral atmosphere (tropospheric refraction), and

$\Delta\rho_{i,ion}^j$ is the delay of the signal due to the ionosphere (ionospheric refraction).

For scientific purposes the phase observable plays a decisive role: At time t_i the phase ϕ_i^j of the received signal is recorded (fractional part). The essential difference of phase vs. code is (a) a much higher precision (rms error of about one millimeter), and (b) an unknown number N_i^j of entire cycles of carrier phase. As the receiver keeps track of the integer number of cycles as a function of time, only one initial phase ambiguity number N_i^j is needed per satellite pass. An additional difference between code and phase concerns the sign of ionospheric refraction: a signal delay corresponds to a phase advance. This leads us to the following phase observation equation:

$$\lambda \cdot \phi_i^j = \rho_i^j - \Delta\rho_{i,ion}^j + \Delta\rho_{i,trop}^j - c \cdot \Delta t^j + c \cdot \Delta t_i + \lambda \cdot N_i^j \tag{2}$$

where N_i^j is the initial phase ambiguity parameter for satellite j and receiver i. Eqns. (2) and (1) immediately reveal the **interdisciplinary potential of the GPS**:

- The geometrical information is contained in the slant range ρ_i^j, which allows us to extract satellite orbits, receiver positions, and Earth Rotation Parameters (ERPs).
- The atmosphere information is contained in the terms $\Delta\rho_{i,ion}^j$ and $\Delta\rho_{i,trop}^j$.
- The satellite and reciever clock information is contained in the terms Δt^j and Δt_i, respectively.

It is essential that each receiver makes measurements to several satellites (ideally to all in view) quasi-simultaneously ("quasi" says that simultaneity can only be achieved apart from (small) receiver and satellite clock errors).

The difference of two quasi-simultaneously acquired pseudoranges by one receiver to two different satellites no longer contains the receiver clock error while the difference of two quasi-simultaneous observations of the same satellite by two receivers i and k (Fig. 2 (right)) no longer contains the satellite clock error. Obviously, a between-satellite and between-receiver difference of observations, a so-called double difference, neither contains satellite nor receiver clock errors. (In the "real world" the influences of these terms are "only" greatly reduced, but not completely eliminated.)

THE INTERNATIONAL GPS SERVICE (IGS)

In the 1980*s* it became clear that the GPS would revolutionize many national, regional, and global tasks in geodesy and geodynamics. The writing was on the wall: Many national geodetic services initiated projects enabling them to "adapt" their highest order networks to the GPS technique. The processing method was differential, the key observable the double difference. For long baselines or big networks the main contributor to the error budget was the orbit error. The rough rule of thumb by Bauersima (1983) states:

$$\Delta\rho_{coord} \approx \frac{l}{d} \cdot \Delta\rho_{orbit}$$

where

$\Delta\rho_{orbit}$ is the error of a satellite position (orbit error),

$\Delta\rho_{coord}$ is the induced (differential) coordinate error,

l is the approximate length of the baseline resp. the diameter of the network, and

$d \approx 20,000$–$25,000$ km is the approximate distance between survey area and the used GPS satellites.

Fig. 3 (left) shows coordinate repeatabilities in latitude, longitude, and height for 90 days in 1994, when analyzing the 1200 km European baseline Graz-Onsala using daily batches of observations and broadcast orbits. Fig. 3 (right) gives the same results in the same scale when replacing broadcast by IGS orbits. According to our rule of thumb we would expect unmodeled orbit errors of about 3 m, which corresponds quite well to the estimated accuracy of the GPS Broadcast Orbits. From Fig. 3 (right) we conclude that the orbit error is virtually eliminated by the IGS orbits.

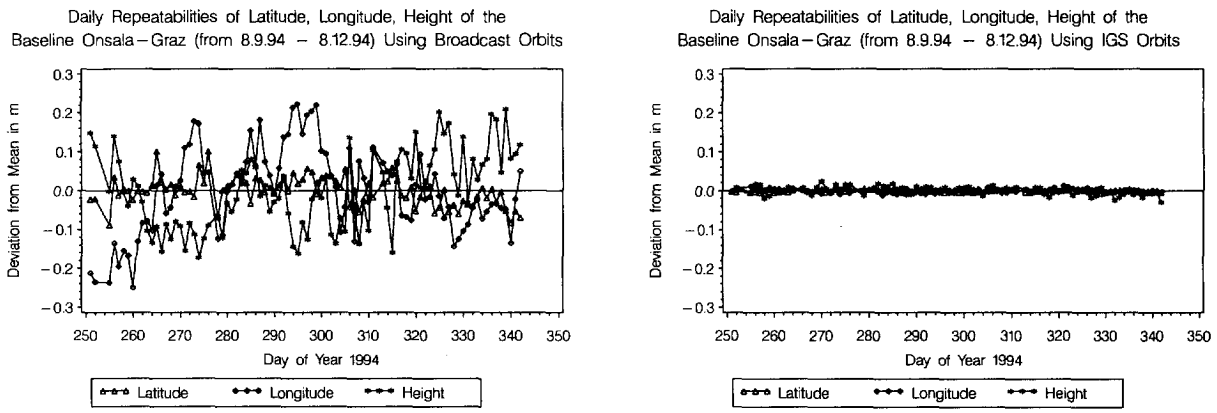

Fig. 3. Geodetic GPS Results using Broadcast and IGS Orbits

Having understood the impact of orbit errors one had to conclude towards the end of the 1980*s*, that each regional or global analysis either would have to improve the GPS orbits or that, alternatively, a scientific GPS (orbit determination) service had to be created. In view of the difficulties associated with orbit determination and with the practical realization of the (global) terrestrial reference frame it was clear that creating a service would be the preferable solution.

Such considerations led to the official creation of the IGS, the International GPS Service, in 1994. Table 1 summarizes the essential steps of the development. Information about the early phase of the IGS may be found in Mueller (1992), the subsequent development is reported, e.g., by Beutler *et al.* (1994, 1996) and Neilan *et al.* (1997).

The 1992 IGS Test Campaign was so successful, that IGS operations never ended, but smoothly went over to the IGS Pilot Service in fall 1992 and to the official IGS in 1994. This means that since 21 June 1992 there is an uninterrupted series of GPS ephemerides and other products available for every calendar day.

The IGS Analysis Workshops in Table 1 were essential for the development of the IGS: The 1993 workshops handled the transition phase from the test campaign to the official service, in the administrative sense in

Bern, in the scientific sense in Ottawa, in the organizational sense in Silver Spring. More information about this phase of the IGS may be found in (Beutler *et al.*, 1994, 1996). The orbit combination procedure is documented in (Beutler *et al.*, 1995). The 1994 workshop in Pasadena saw the creation of the IGS Pilot Project for the Densification of the ITRF (International Terrestrial Reference Frame, Boucher *et al.* (1996)) using GPS Regional Networks. The result of this effort eventually will consist of a set of coordinates and velocities for 200 globally well distributed sites. This IGS Polyhedron with coordinate accuracies of better than 1 cm and velocity accuracies better than 1 mm/year is an important product for the user community.

Table 1. Chronicle of IGS Events 1989–1998

Date	Event
Aug 89	I.I. Mueller, G. Mader, W.G. Melbourne, B. Minster, and R.E. Neilan present first ideas at the IAG General Meeting in Edinburgh
Mar 90	Creation of IGS Planning Committee
Aug 91	Planning Committee reorganized and renamed IGS Campaign Oversight Committee
Jun 92	Start of 1992 IGS Test Campaign (ended 23 Sep 1992)
Nov 92	Start of IGS Pilot Service
Mar 93	Analysis Center Workshop in Bern
Sep 93	Analysis Center Workshop in Ottawa
Sep 93	Network Workshop in Silver Spring
Jan 94	Start of official IGS
Nov 94	Workshop on Densification of the ITRF in Pasadena
May 95	Workshop Special Topics and New Directions in Potsdam
Mar 96	Analysis Center Workshop in Silver Spring
Mar 97	Analysis Center Workshop in Pasadena
Dec 97	IGS Retreat 1997 in San Francisco
Feb 98	1998 IGS Analysis Center Workshop in Darmstadt

The extension of the IGS to Atmosphere Sciences and to Low Earth Orbiting Satellites (LEOs) carrying GPS receivers was first discussed at the 1995 IGS Workshop in Potsdam, then at the 1996 and 1997 workshops and led to the creation of the IGS LEO Working Group and of the IGS Troposphere Combination Center at GFZ (GeoForschungsZentrum in Potsdam) in 1997, and to the creation of the IGS Ionosphere Working Group in 1998. Moreover, at the *8th* IGS Governing Board Meeting in December 1997 the IGS/BIPM Project to Study Accurate Time and Frequency Comparisons was created, where the attempt is made to exploit the IGS network (and to extend it in a meaningful way) for the purpose of high accuracy time and frequency transfer.

The essential components of the IGS are (a) its global network (present configuration with about 200 stations in Fig. 4) (b) global and regional IGS data centers, (c) IGS analysis centers, (d) the IGS analysis coordinator, and (e) the IGS central bureau.

More information concerning the present structure of the IGS and the estimated accuracies of its products may be found in Neilan *et al.* (1997) and in the IGS Colleague Directory (Neilan *et al.*, 1998). For an update on recent achievements of the IGS we refer to the IGS Annual Reports, e.g., to Zumberge *et al.* 1997.

IGS ORBIT INFORMATION

Since the start of the official service in 1994 the IGS Final Orbits were produced and made available through the IGS Analysis Coordinator based on the contributions from the seven IGS Analysis Centers (three centers,

namely CODE, ESA, GFZ, in Europe, three, namely JPL, NGS, and SIO, in the U.S., and one, EMR in Canada).

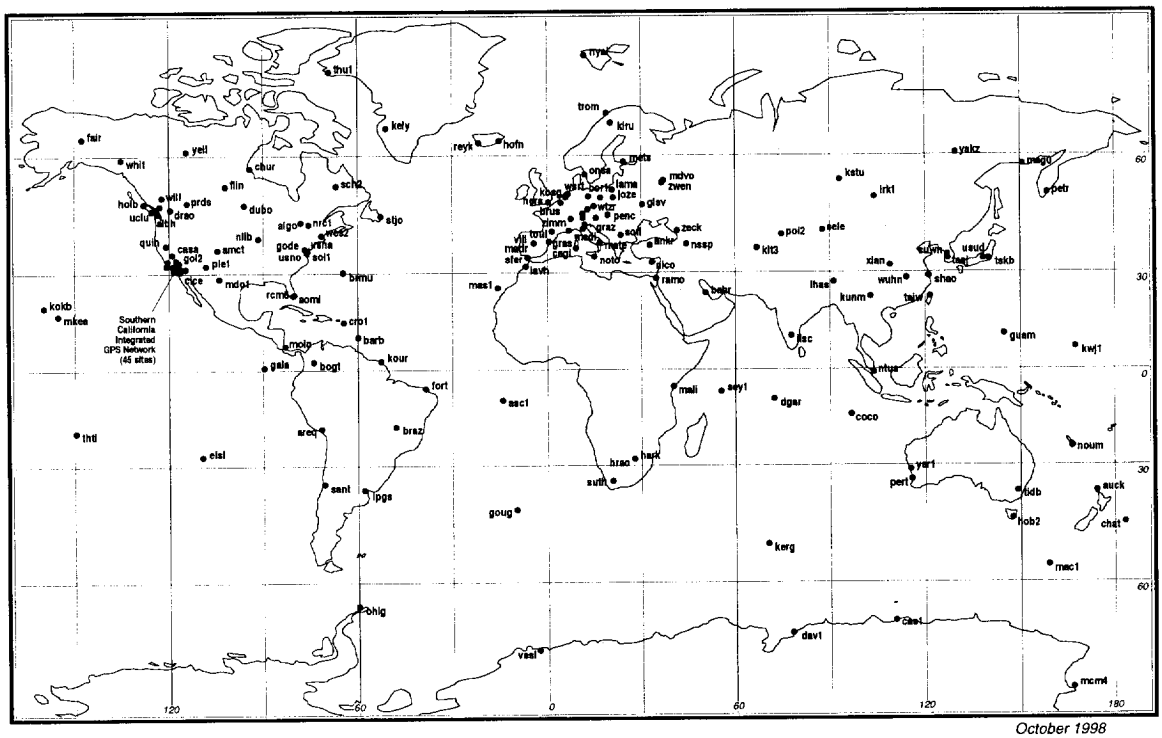

Fig. 4. The GPS Tracking Network of the IGS in 1998

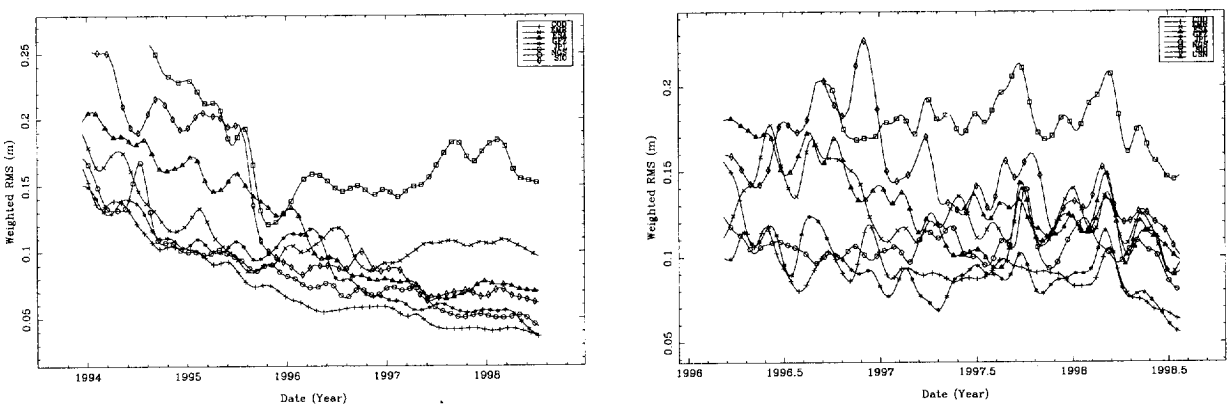

Fig. 5. Consistency of IGS Final and Rapid Orbits (smoothed RMS values)

The IGS Final Orbits are made available with a delay between 10 to 12 days. This is the orbit information that should be used if highest accuracy is required (first order networks, regional geodynamics projects, etc.).

Fig. 5 (left) shows the consistency of the contributions to the IGS Final Orbit as delivered by the seven IGS Analysis Centers: the mean weekly rms-values w.r.t. the IGS final orbit are given as a smoothed function of time for each Analysis Center and for each week since the end of 1993. One can see that most Centers have reached a consistency of several centimeters rms. Using the IGS orbits to compute distances measured by Satellite Laser Ranging (which is only possible for two satellites equipped with laser reflectors) indicates that this consistency is close to the accuracy for the IGS orbits as well. Fig. 5 and our rule of thumb tell us that the orbit error has become negligible in the error budget of the GPS observable!

There was considerable pressure on the IGS to make available its products with a shorter delay (than 12 days for the final orbit). This is why in 1996 the IGS Analysis Center Coordinator started producing the IGS Rapid Orbit which is available to the user with a delay of only about one day. Fig. 5 (right) shows that the IGS Rapid Orbit consistency is slightly inferior to the consistency of the IGS final orbits. The quality difference is explained by still existing problems of data availability. The improvement in 1998 is attributed to the much improved data availability. IGS Rapid Orbits are extensively used by the atmosphere community for the computing the water vapour content of the atmosphere (see below).

POLAR MOTION AND UNIVERSAL TIME

Fig. 6 shows (in essence) the motion of the Earth's rotation axis on the surface of the Earth as seen by the IGS. The IGS Analysis Centers (AC) generate Earth Rotation Parameters (ERPs) and orbits in the same parameter estimation process and the Analysis Coordinator preserves this consistency in the combined orbits and pole. The daily IGS pole coordinates x and y are accurate to about 0.1 milliarcseconds (mas) for the final, and to about 0.2 mas for the rapid IGS products (corresponding to 3–6 mm on the Earth's surface)! IGS products are of comparable quality as the corresponding estimates of the other space geodetic techniques (in particular Satellite laser Ranging (SLR) and Very Long Baseline Interferometry (VLBI)), but the temporal resolution (one data point per day) for regular IGS products is unique.

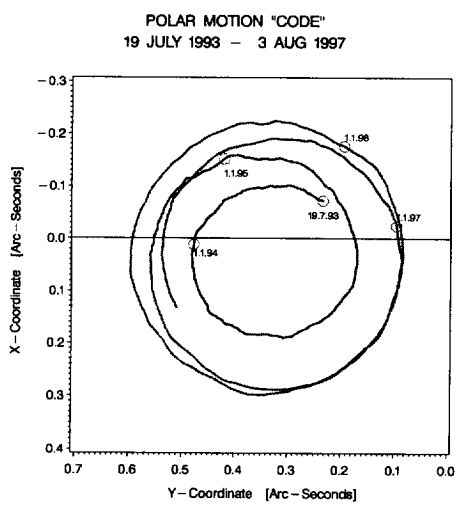

Fig. 6. Polar Motion as Established by one of the IGS Analysis Centers

GPS, as a satellite geodetic technique, is not able of measuring Universal Time (UT), as realized through the Earth's rotation. This is due to the high correlation between UT and the orbital elements of the satellites. GPS is capable, on the other hand, to measure the rate of rotation of the Earth. The rotation rate is the first time derivative of UT. Fig. 7 shows the IGS-derived length of day (LOD) values (rotation rates expressed as excess of revolution periods) for the entire series of IGS final products.

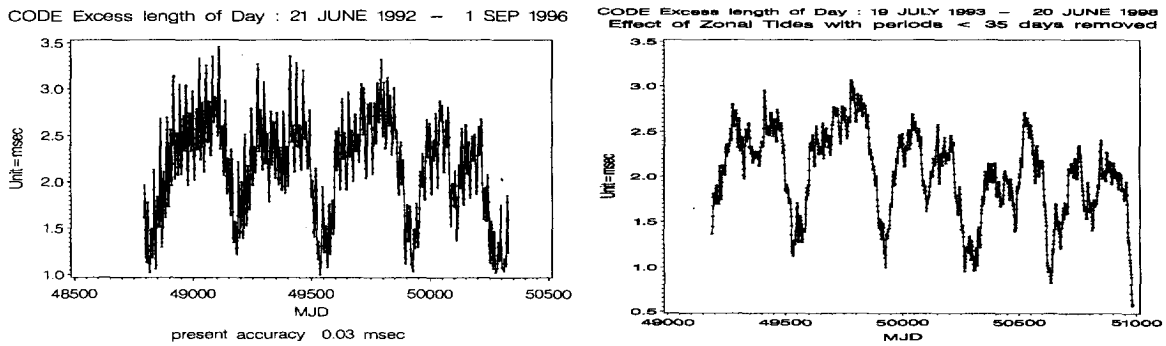

Fig. 7. Excess Length of Day, Daily Values estimated by an IGS Analysis Center

Fig. 7 (left) contains raw LOD values, Fig. 7 (right) LOD values after removal of tidal effects with periods shorter than 35 days.

Figs. 6 and 7 clearly show that the angular momentum of the Earth is changing (otherwise the length of day would be constant and polar motion would be circular with uniform angular velocity). It is thus possible to compute the total angular momentum of the Earth (without the atmosphere) using polar motion data and LOD data. One may show that the first two components of angular momentum are a function of polar motion only, whereas the third is function of LOD (rotation rate of the Earth).

Where do the changes of angular momentum come from? Let us compare the changing angular momentum functions χ_1, χ_2, and χ_3 (which are scaled versions of the angular momentum) of the Earth as computed from our IGS polar motion and length of day data and compare the result with the Atmospheric Angular Momentum (AAM) as computed by the AAM Sub-bureau of the IERS using meteorological data (pressure, temperature, wind, etc., from global meteorological networks) see e.g. , Salstein (1997). Fig. 8 shows the two equatorial components of the angular momentum as computed from IGS and from AAM data for the year 1997. Obviously, both series are highly correlated (correlation coefficient of about 0.5–0.7). We conclude that the Earth's atmosphere is to a high degree responsible for the irregularities of polar motion.

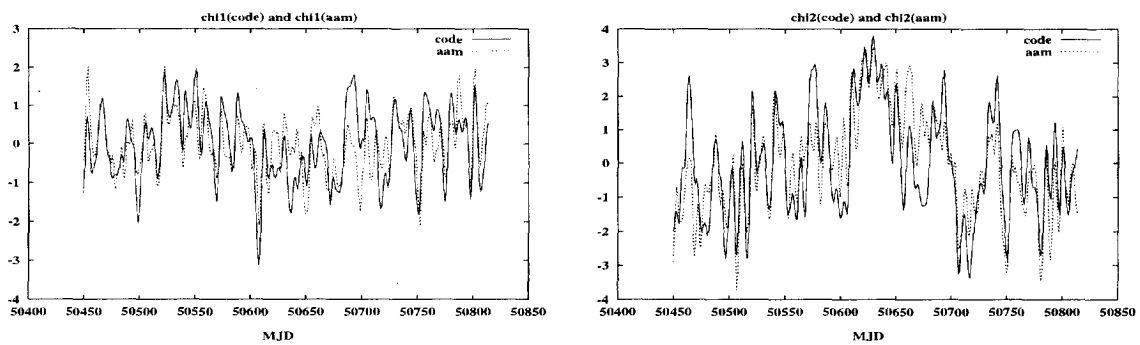

Fig. 8. First and Second Angular Momentum Functions χ_1 and χ_2 computed from IGS and AAM data in non-dimensional units of 10^{-7}

The correlation is even more striking for the third component: Fig. 9 (left) gives the two sets of angular momentum for a time period of about five years, Fig. 9 (right) for the year 1997. The correlation of the two time series is about 0.95!

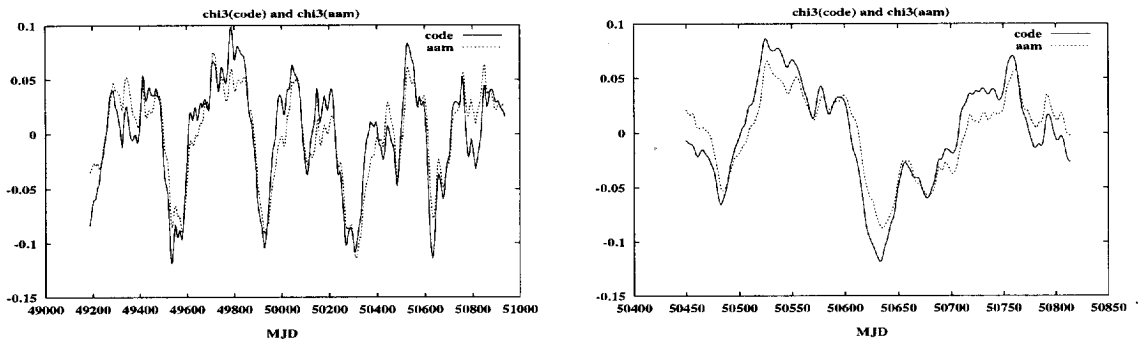

Fig. 9. Third Component of Angular Momentum Function χ_3 computed from IGS and AAM data in non-dimensional units of 10^{-7} (zonal tides with periods shorter than 35 days removed)

This high degree of correlation was not detected by GPS or by the IGS. Barnes *et al.* (1983) established it already in 1983 using VLBI data. However, the IGS for the first time confirmed the correlation for the χ_1 and χ_2 components for periods shorter than about ten days. Today, the IGS is in a position to provide a long, consistent, and dense set of space geodetic polar motion and LOD series.

IGS REALIZATION OF THE TERRESTRIAL REFERENCE FRAME

The IGS, through its Analysis Centers, significantly contributes to the realization of the ITRF, the International Terrestrial Reference Frame, as established by the IERS, the International Earth Rotation Service, a multi-technique global reference frame. We refer to the Technical and Annual Report series of the IERS for more information.

The individual solutions and the final "result" consist of sets of station coordinates and velocities. Fig. 10 illustrates a velocity solution of the GFZ Analysis Center of the IGS based on about five years of data.

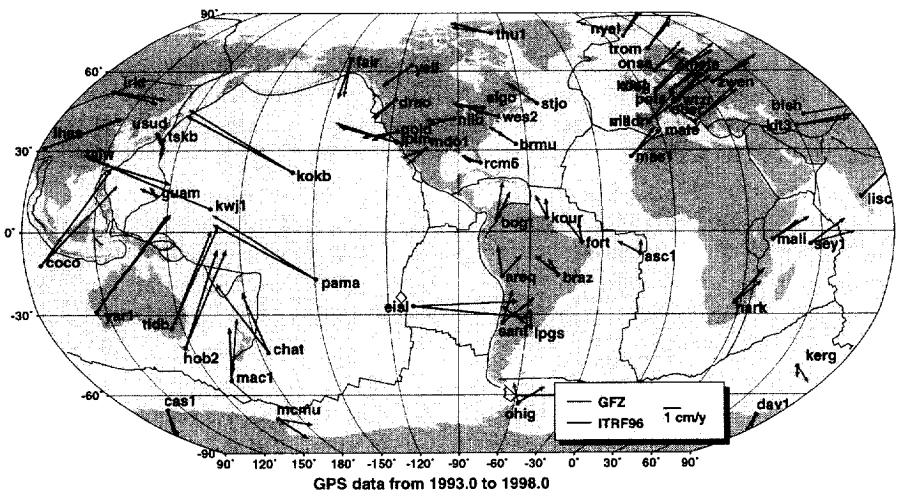

Fig. 10. Station Motion as computed by the GFZ Analysis Center

Combining the results of all seven IGS Analysis Centers and of all IGS Regional Associate Analysis Centers will lead to a self-consistent IGS realization of the ITRF in the near future.

Fig. 11 shows the temporal evolution of the coordinates (north, east, and up components) of two sites in Belgium (Dourbes and Dentergem). IGS velocity estimates are based on such (daily) coordinate estimates. Figs. 11 illustrate that there is not only a secular motion, but that there are signals with longer periods involved.

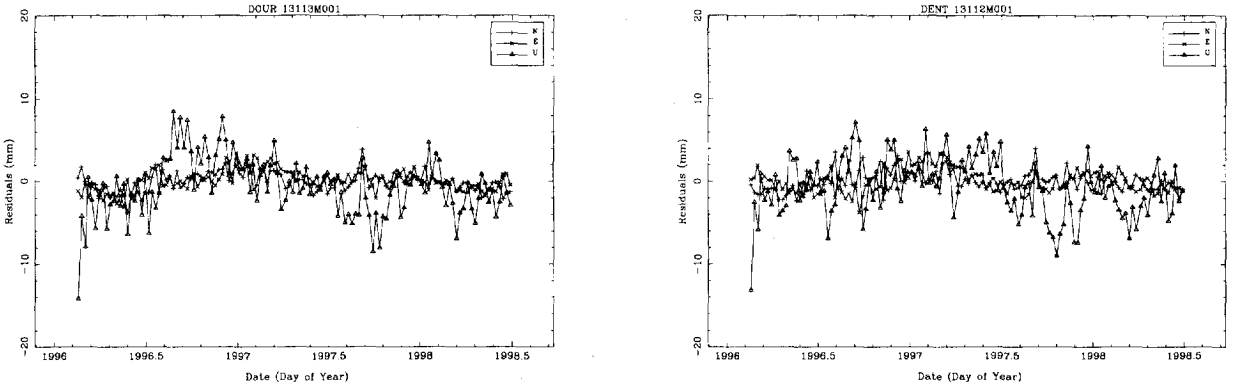

Fig. 11. Daily Positions of Stations Dourbes and Dentergem in Belgium

It will be one of the "hot" research topics of the near future to find out whether such variations are real and how they can be interpreted. Such analyses will have to consider solutions of all space geodetic techniques.

EARTH ROTATION: ADVANCED ASPECTS

Let us look here into some of the more advanced IGS products using, however, the same observations as in standard IGS processing. We discuss (a) determination of nutation terms using *IGS*-data; (b) polar motion with a higher time resolution (two hours instead of one day). Generalization (b) is straight forward, whereas generalization (a) asks for a few comments.

In astronomy we make the distinction between the motion of the Earth's rotation axis on the surface of the Earth and the motion of the Earth's axis in inertial space ("motion among the stars"). The former motion is called polar motion and was already addressed, the latter motion is called precession and nutation, where the distinction is somewhat artificial.

Precession plus nutation in longitude Ψ, nutation in obliquity ϵ, and sidereal time Θ are illustrated in Fig. 12. The three Eulerian angles are required to describe the body-fixed coordinate system in inertial space. Sidereal time essentially is $\kappa \cdot UT1$ (the angle between the Greenwich meridian and the vernal equinox measured in the equatorial plane; $\kappa \approx 366.25/365.25$ takes into account the ratio between the solar and the sidereal time scale).

The three angles vary in time, by far the fastest motion being that in sidereal time Θ (revolution period of one day, as opposed to a revolution period of precession of about 26,000 years). From the mathematical point of view there are no differences in principle between the three Eulerian angles.

We have mentioned that satellite geodetic methods cannot establish UT1 but only length of day. A similar statement holds for nutation: satellite geodetic techniques have no access to nutation in longitude and obliquity, but to the time derivative of these quantities.

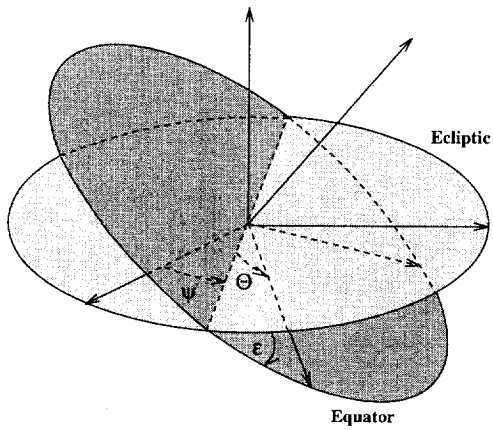

Fig. 12. Earth-Fixed and Inertial Reference Systems Connected Through the Three Eulerian Angles

This principle was followed by Rothacher *et al.* (1998a) to estimate nutation amplitudes for short period nutation terms based on three years of daily $\dot{\Psi}$ and $\dot{\epsilon}$ values. The authors first analysed the potential of the method and compared it to the achievements of today's state of the art technique, namely VLBI. Fig. 13 shows that the formal errors of the two methods differ significantly: whereas for VLBI the error is (almost) not depending on the period of the particular nutation term, GPS is performing in an excellent way, as a matter of fact better than VLBI, for short period terms, but becomes virtually useless for terms of periods longer than, let us say, one month.

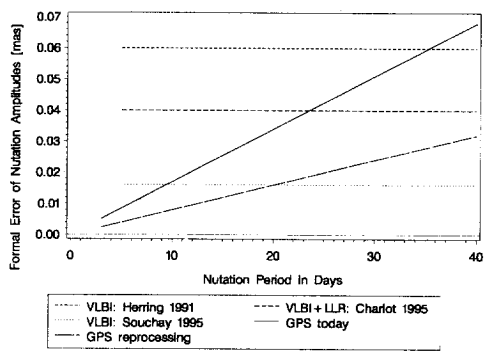

Fig. 13. Formal Errors of Nutation Terms as Estimated by GPS and VLBI (from Rothacher *et al.* (1998a))

The solid GPS-line represents the errors as they were encountered in the analysis performed by Rothacher *et al.* (1998a), the dashed GPS-line is a conservative estimate for the error if the entire time series of three years were reprocessed with the latest software tools. Fig. 13 confirms that there is no long term stability of the GPS-defined inertial frame, but that short-term stability is excellent. The middle of the VLBI error lines is a conservative, the lower a rather optimistic VLBI error assessment.

Fig. 14 shows amplitude spectra of the GPS-established (left) and VLBI-established (right) nutation series (nutation terms in longitude and obliquity decomposed into prograde and retrograde terms with positive and negative periods) relative to the IERS 1992 model (see IERS conventions 1996, McCarthy (1996)). It should be mentioned that Fig. 14 (left) stems from actual GPS measurements, whereas Fig. 14 (right) is based on the difference between the IERS 1996 model computed from about 20 years of VLBI observations

and the IAU 1980 model. Despite these differences we see that both spectra show essentially the same signature — which indicates that both the VLBI and GPS techniques see the same reference frame.

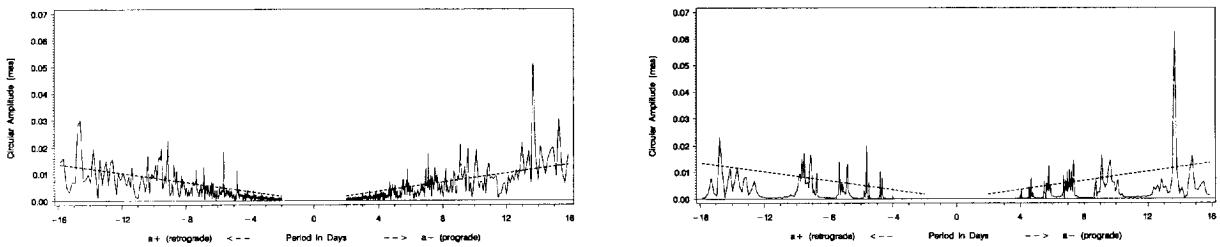

Fig. 14. Nutation Terms of GPS solution and of IERS 1996 model (established by VLBI) Relative to IAU 1980 Model

Fig. 15 compares the GPS nutation results to the IERS 1996 model. It can be said that the agreement is excellent. The results should (hopefully) stimulate a common evaluation of VLBI and GPS nutation series. The shaded area gives the 2-σ error of the GPS method.

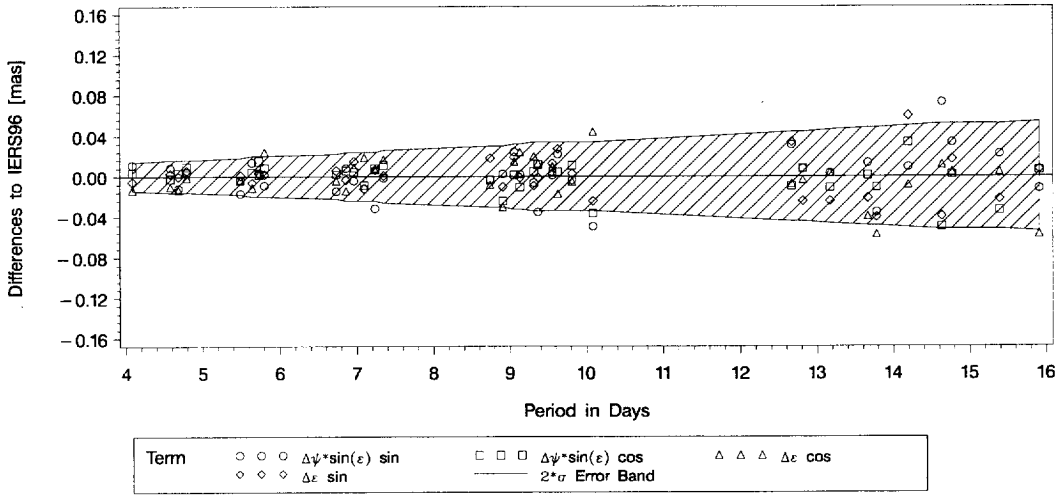

Fig. 15. GPS-Derived Nutation Terms compared to VLBI-Derived Nutation Series

Let us close this section by looking at some results derived from polar motion analyses using a high time resolution. The results, taken from Rothacher (1998b), are based on about three years of high resolution ERP-values (two-hour estimates for polar motion and for UT) extracted from the CODE Analysis Center of the IGS. The spectral analyses in Fig. 16 show sharp peaks in the prograde and retrograde diurnal and semidiurnal bands (the retrograde diurnal band (top, right) is an exception: due to correlations with the orbit elements such terms may not be estimated by GPS). The peaks are associated with the expected frequencies of ocean tides (for experts: the tidal waves are marked in Fig. 16).

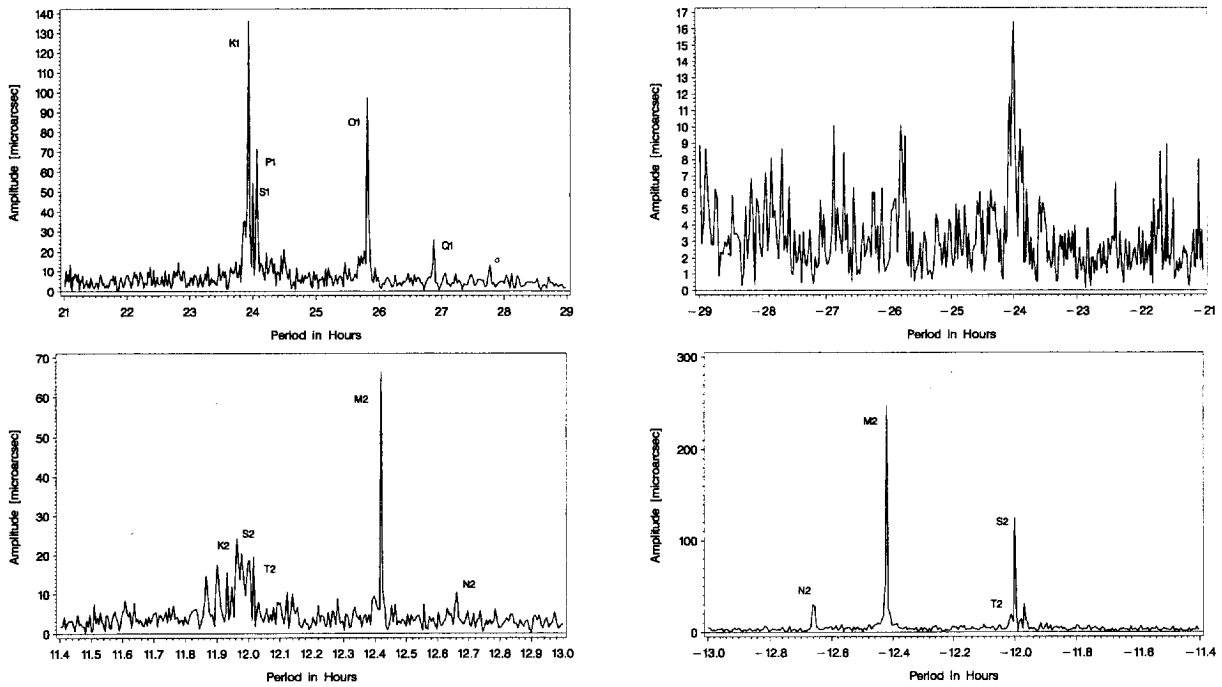

Fig. 16. Spectra of Diurnal and Semidiurnal Prograde (Positive Periods) and Retrograde (Negative Periods) Polar Motion Established by GPS

Fig. 17 gives the corresponding results for the length of day estimates. Again we see sharp peaks corresponding to the diurnal and semidiurnal retrograde band.

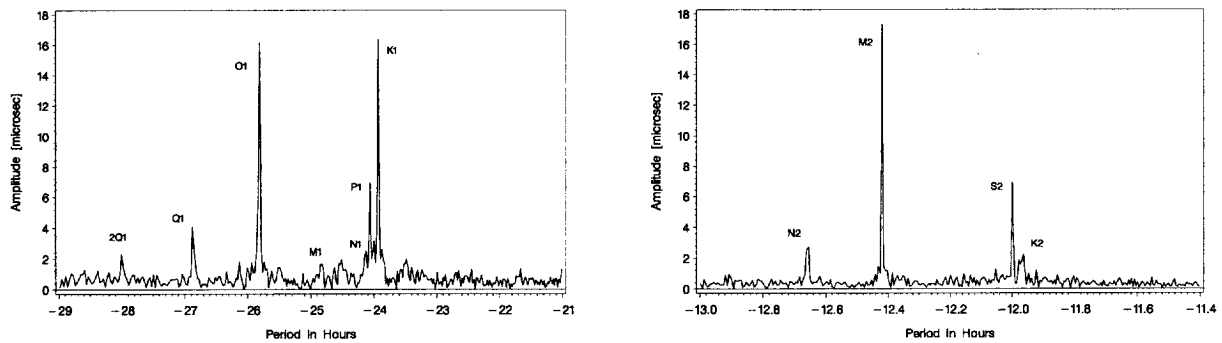

Fig. 17. Spectra of Diurnal and Semidiurnal Retrograde LOD Variations

That the results established by Rothacher (1998b) are of excellent quality is also apparent in Fig. 18 where, for a short time interval, the GPS measured LOD values (solid lines) are compared to the latest model for polar motion due to ocean tides as it was established by Ray (1994). This model is based on TOPEX/POSEIDON altimetry data and is probably the best available today.

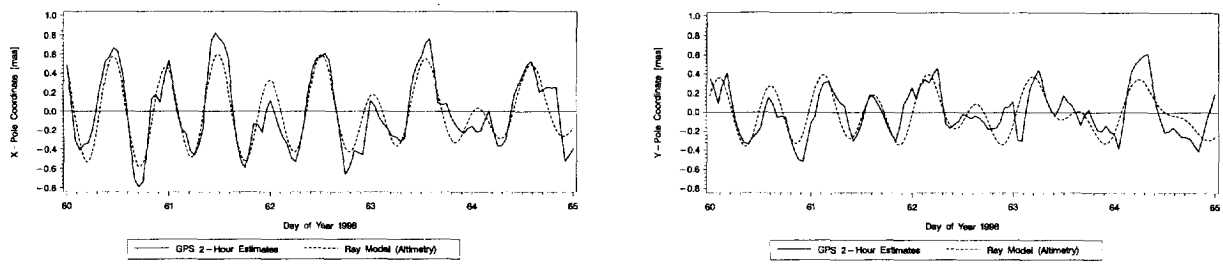

Fig. 18. Comparison of a GPS Measurement Series and an Ocean Tide Model Derived From Topex/Poseidon Altimetry

EXPLOITING THE IGS NETWORK FOR ATMOSPHERE MONITORING

Ionosphere Monitoring

GPS satellites transmit signals on the two carriers $L1$ and $L2$ through the Earth's atmosphere. The two carriers allow it to eliminate, or, alternatively, to determine ionospheric refraction which is frequency dependent:

$$\Delta\rho_{ion,L1} = \frac{\alpha}{\nu_{L1}^2} \cdot E$$

$$\Delta\rho_{ion,L2} = \frac{\alpha}{\nu_{L2}^2} \cdot E$$

ν_{Li} is the frequency associated with carrier Li, E is the integrated number of free electrons in the rotational cylinder of unit ground surface between receiver and satellite, usually designated as total electron content (TEC), and $\alpha = 40.3$ ms^{-2}TECU^{-1} is a numerical constant. The above formula actually is only an approximation, but higher order terms are so small that usually they may be neglected. Introducing the above relations into the observation equations for the code observable (1) we obtain:

$$\begin{aligned} p_{i,L1}^j &= \rho_i^j + \frac{\alpha}{\nu_{L1}^2} \cdot E + \Delta\rho_{i,trop}^j - c \cdot \Delta t^j + c \cdot \Delta t_i \\ p_{i,L2}^j &= \rho_i^j + \frac{\alpha}{\nu_{L2}^2} \cdot E + \Delta\rho_{i,trop}^j - c \cdot \Delta t^j + c \cdot \Delta t_i \end{aligned} \tag{3}$$

A similar set of equations may be established for the phase observation equations. Eqns. (3) (and the corresponding equations for the phase) are fundamental for GPS processing strategies. By multiplying the first of equations (3) by $\frac{\nu_{L2}^2}{\nu_{L1}^2 - \nu_{L2}^2}$, the second by $\frac{\nu_{L1}^2}{\nu_{L1}^2 - \nu_{L2}^2}$ and then by subtracting the two equations, we obtain an artificial code observable, the so-called ionosphere-free linear combination of the two original observables, where ionospheric refraction is eliminated. It is the standard observable for all high-accuracy applications for regional and global applications except when the ionosphere itself is the target of investigations.

In the latter case we can form the geometry-free linear combination of the two equations (3), which is the plain difference of eqns. (3):

$$p_{i,L1}^j - p_{i,L2}^j = \alpha \cdot E \cdot \left[\frac{1}{\nu_{L1}^2} - \frac{1}{\nu_{L2}^2}\right] \tag{4}$$

Eqn. (4) neither contains geometrical nor clock information. In actual analyses one has to take into account differential code biases between the $L1$ and the $L2$ code observables. We refer, e.g., to Manucci *et al.* (1994), Feltens *et al.* (1998), and Schaer *et al.* (1998a) for more information. The geometry-free observation equation for the phase contains an additional term due to the ambiguity parameters N_{L1} and N_{L2} in $L1$ and $L2$, and the sign of ionospheric refraction is opposite:

$$\lambda_{L1} \cdot \phi_{i,L1}^j - \lambda_{L2} \cdot \phi_{i,L2}^j = -\alpha \cdot E \cdot \left[\frac{1}{\nu_{L1}^2} - \frac{1}{\nu_{L2}^2}\right] + (\lambda_{L1} \cdot N_{L1} - \lambda_{L2} \cdot N_{L2}) \tag{5}$$

Eqns. (4) and (5) are the observation equations for mapping the ionosphere. When establishing regional and/or global ionosphere maps one usually makes the simplifying assumption that all free electrons are contained in a single layer in a height H above the surface of the Earth. In this case the electron content E, as seen by a particular receiver, may be expressed by the single layer density E_s at the piercing point of the line receiver-satellite and by the zenith distance z' of this line at the ionospheric pierce point. The model is illustrated in Fig. 19.

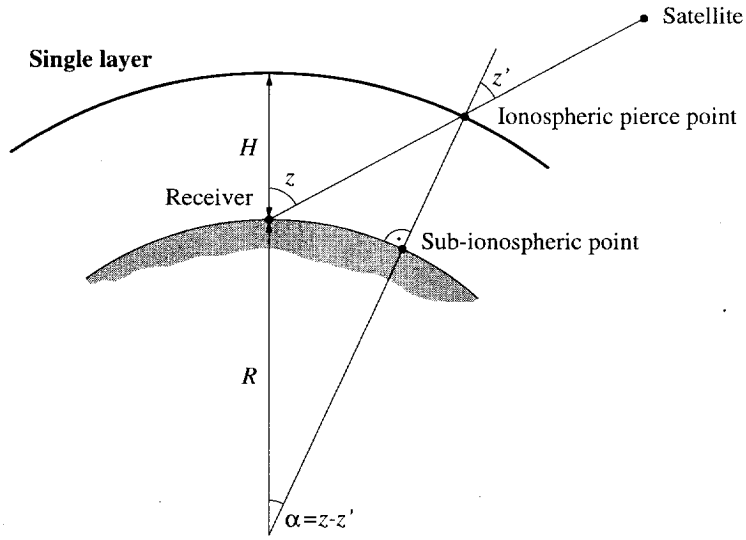

Fig. 19. Single Layer Model for the Earth's Ionosphere

In the single layer ionosphere model we may put

$$E = \frac{E_s}{\cos z'},$$

to convert the line-of-sight TEC E to the vertical TEC E_s. Then we introduce this equation into eqns. (4, 5)to compute the surface density E_s on the sphere, *e.g.*, as a truncated development of spherical harmonics or as latitude and longitude dependent surface densities. As a matter of fact very different mathematical models are used by the experts in the field. It was therefore a constructive achievement of the IGS Ionosphere Working Group that the IONEX-Format, the Ionosphere Map Exchange Format, was developed, which allows it to compare ionosphere maps, which are described by very different mathematical models (Schaer *et al.* 1998b).

Figs. 20 show ionosphere maps as they were produced by the JPL Ionosphere Associate Analysis Center (IAAC) of the IGS. It is a subset of four maps (corresponding to 02:30 UT, 08:30 UT, 14:30 UT, and 20:30 UT) of originally 24 hourly maps corresponding to June 1, 1998. One can easily follow the rotation of the "bulge" of the electron distribution along the geomagnetic equator (dotted line in Figs. 20); one can also see the bifurcation of the bulge in the equatorial regions. Similar maps were produced by other IAACs. The particular example marks, by the way, the beginning of the IGS Ionosphere comparison and combining activities.

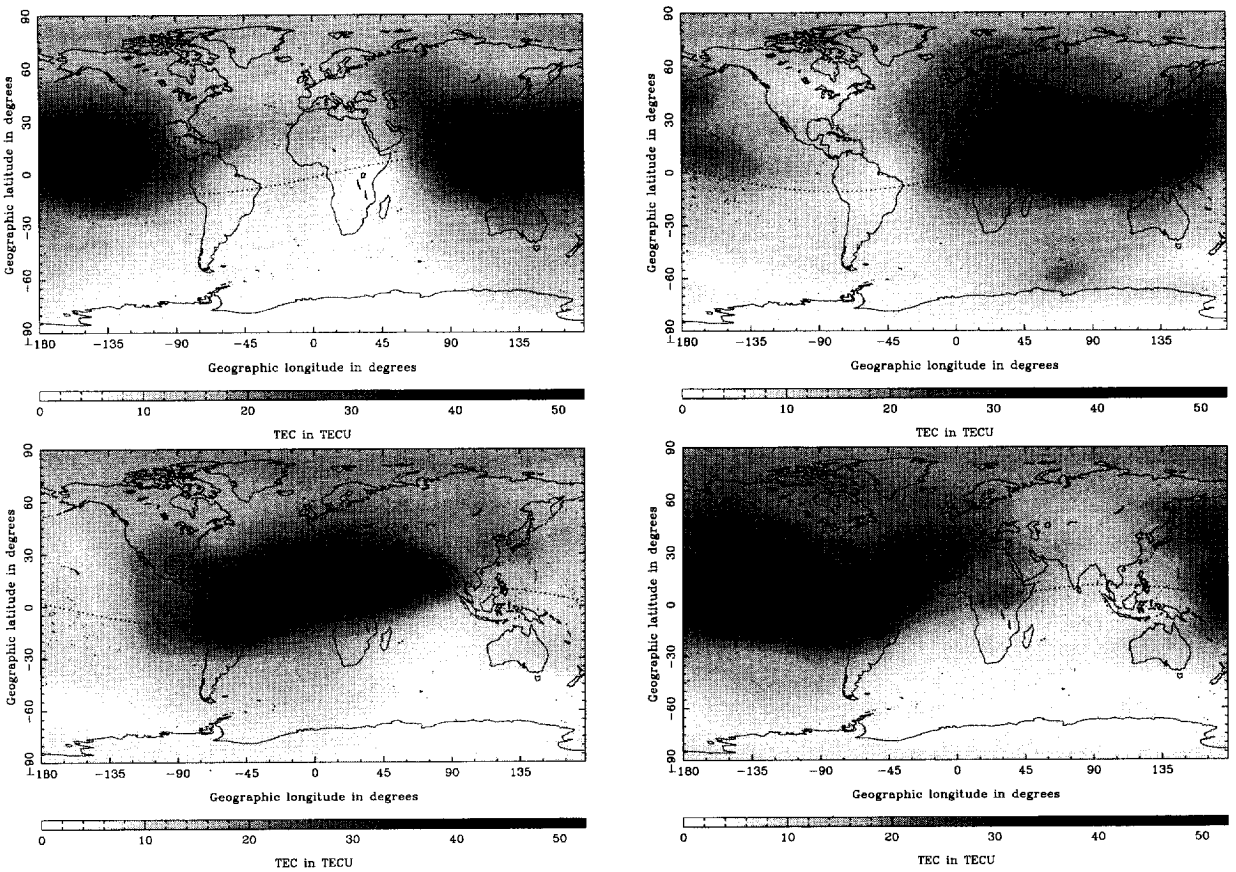

Fig. 20. Ionosphere Maps of the JPL IAAC Referring to June 1, 02:30 UT (top, left), 08:30 UT (top, right), 14:30 UT (bottom, left) and 20:30 UT (bottom, right)

Some of the groups collaborating now in the IGS Ionosphere Working Group already have a long record of ionosphere related activities. Fig. 21 shows the mean and maximum TEC for the time period from January 1, 1995 to end of June, 1998 as established by the CODE IAAC (see Schaer *et al.* (1998a)). Fig. 21 may be considered as an IGS-documentation of the most recent period of low solar activity. Unnecessary to say, that the development will be much more exciting in the years of high solar activity.

Let us conclude by indicating why global ionosphere mapping using the IGS network is so successful. From Fig. 19 we may conclude that one single station, observing with a maximum zenith distance of $z_{max} \approx 80^o$, has access to a geocentrical "cap" of radius

$$\alpha_{max} = z_{max} - z'_{max} = z_{max} - \arcsin\left\{\frac{R}{R+H} \cdot \sin z_{max}\right\} \approx 13.1^o \tag{6}$$

Each station of the IGS network thus has access to a spherical cap with a geocentric radius of about α_{max} (where we used $R \approx 6370$ km for the Earth radius and $H \approx 450$ km for the height of the single layer). Our result in turn implies that the entire single layer might be monitored by about 80 well distributed sites. This corresponds about to the present number of global IGS sites – unfortunately we see in Fig. 4 that the distribution is far from ideal for our purpose.

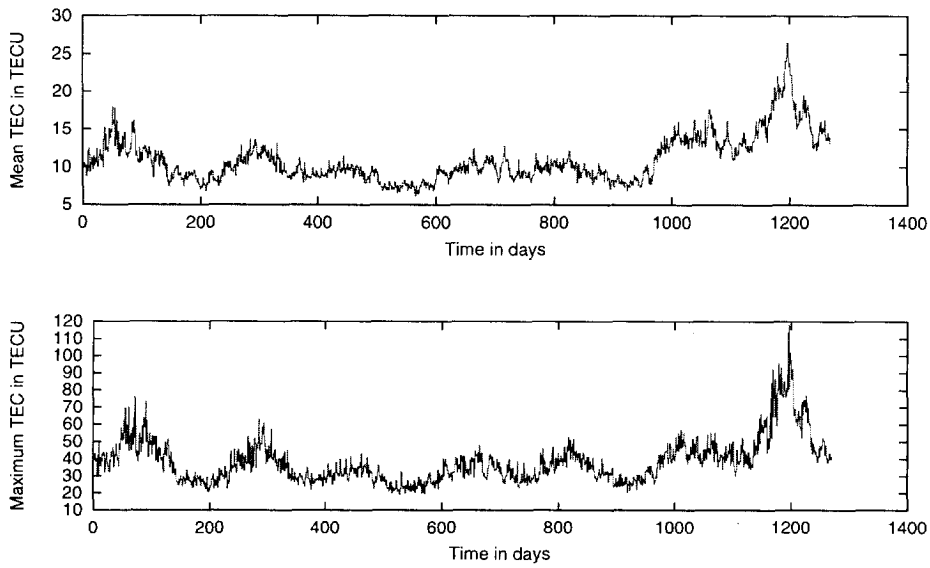

Fig. 21. Daily Mean and Maximum Total Electron Content since 1 January 1995

Troposphere Monitoring

In this section we deal with the term $\Delta\rho^j_{i,trop}$ in the GPS observation equations (1) and (2). The importance of this term was underestimated in the pioneer days of high accuracy GPS applications (beginning of the 1980*s*) when mainly very short baselines with small height differences ("parking lot demonstrations") were analysed to prove the usefulness of the GPS. It was really only after the elimination of the orbit error thanks to the IGS that tropospheric refraction was recognized to be the principal accuracy limiting factor of the GPS. The same statement is of course true for all techniques in the microwave band like, e.g., VLBI. As a matter of fact, many troposphere-related studies in GPS applications were stimulated by VLBI analyses.

To assess the order of magnitude we mention that in the zenith direction the path delay $\Delta\rho^j_{i,trop}$ of a GPS signal due to the troposphere is of the order of 2.2–2.6 meters for a station at sea level. Variations of up to 10 centimeters within two hours are not exceptional. This is why IGS Analysis Centers solve (at least) for one troposphere parameter per 2-hour time interval, or, what is preferable for this kind of signal, model tropospheric refraction as a stochastic process.

Tropospheric refraction in the microwave band is wavelength-independent and it may show a high temporal variation. Let us write it in the form:

$$\Delta\rho^j_{i,trop} = \Delta\rho_{i,hyd} \cdot m^j_{hyd,i}(z) + \Delta\rho_{i,wet} \cdot m^j_{wet,i}(z) \tag{7}$$

where $\Delta\rho_{i,hyd}$ is the hydrostatic, $\Delta\rho_{i,wet}$ is the wet delay in zenith direction, $m^j_{hyd,i}$ and $m^j_{wet,i}$ are the corresponding "hydrostatic" and "wet" mapping functions to compute the delay in the zenith distance z, in which the satellite j is seen from station i. In eqn. (7) it is assumed that there are no horizontal gradients of tropospheric refraction.

The hydrostatic delay is due to the pressure of dry air (and due to the partial water vapor pressure). A delay of the same magnitude is also observed, e.g., in the optical band of the electromagnetic spectrum. The hydrostatic or dry component may very well be taken into account, if high precision barometers (and

thermometers) are deployed at the receiver sites. The high temporal variation is mainly due to the wet tropospheric delay. This delay is caused by a resonant interaction of the radiation in the microwave band with water molecules in the atmosphere. It is this wet component which forces GPS and VLBI analysts to estimate tropospheric refraction parameters in their analyses.

Until the early 1990*s* tropospheric refraction was considered a nuisance in GPS processing. Bevis *et al.* (1992) were the first to realize the potential of the GPS for meteorological research. They pointed out that the Integrated Precipitable Water Vapor (IPWV) in a vertical column of unit surface above a station may be (approximately) computed by

$$IPWV \doteq a \cdot \Delta\rho_{wet} \tag{8}$$

where $a \approx \frac{1}{6}$. Now, GPS estimates give very accurate estimates for the total zenith delay (with a high temporal resolution), precise barometers (and thermometers) deployed at the sites allow it to remove the hydrostatic delay, thus leaving us with the wet delay. Using eqn. (8) we obtain the total precipitable water vapor content over each of the stations in an analysis.

Fig. 22 gives insight into the power of the method. It displays time series of (total) tropospheric zenith delays as established by the CODE IGS Analysis Center for a time interval of almost four years for three IGS stations. The original time series were corrected to refer all to sea level and are thus comparable. We can see that the equatorial (and coastal) site Kourou (near the ESA launch site in South America) has the highest, the Antarctic site McMurdo the smallest mean tropospheric zenith path delay (ZPD). Both of these time series show almost no annual variation. The short period variations are significantly larger for the equatorial site. The mid-latitude site in Zimmerwald (Switzerland) on the other hand shows a clear annual signal (maxima in summer, minima in winter).

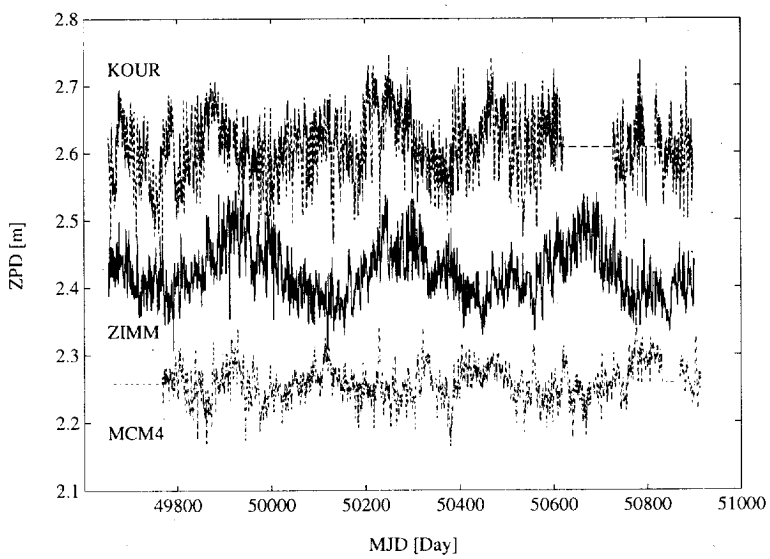

Fig. 22. Estimation of Tropospheric Refraction (Time Resolution of Six Hours) for the IGS Stations Kourou (Equatorial Region), Zimmerwald (Mid-Latitude), and McMurdo (Antarctic)

The characteristics of the ZPD time series is dominated by the wet component: The equatorial site is near the coast and has a very high average water vapour content. The periodic variations are rather large. The mid-latitude site shows a strong annual signal — confirming that warm air will contain more humidity.

Intuition and experience tells that weather, in particular in mountainous areas, may be rather local (as opposed to regional or global) in character. Moreover, a single GPS receiver overviews only a small portion of the Earth's troposphere. Let us assume — to assess the order of magnitude — that tropospheric refraction is due to a layer in a height of five kilometers. Using eqn. (6) we see that a single station has only access to a spherical geocentric cap with a radius of about 0.25^o. In order to get a global coverage of the troposphere comparable to that of the ionosphere we would need a receiver density which is about $(13.1/0.25)^2 \approx 2700$ times higher. As opposed to about 80 globally well distributed receivers (to get sound ionosphere maps) we would need more than 200,000 GPS receivers to obtain good global troposphere maps, a number which is completely out of the question — even if we take into account that we might not need complete coverage over deserts and other uninteresting areas, meteorologicaly speaking.

Nevertheless, GPS for climatological purposes and for weather predictions is of vital importance in regions of particular interest for meteorology or in areas where dense GPS arrays are available for other purposes. Let us mention in this context the GPS array of 1000 receivers distributed over the Japanese islands which is perfectly well suited for such applications of the GPS.

Where lies the contribution of the IGS for such regional applications? The answer is clear:

- IGS rapid and predicted orbits (and the associated information like clocks, earth orientation parameters) and IGS predicted orbits are used by the meteorologists to generate their results.
- IGS time series of tropospheric zenith delays with a time resolution of two hours which are available through the IGS Troposphere Comparison and Coordination Center at GFZ in Potsdam play the role of benchmarks and should be used for absolute calibration of troposphere estimates extracted from regional networks.

NEW DEVELOPMENTS

Time and Frequency Transfer

Specialized GPS timing receivers are available and have been used for a long time. Such receivers are single frequency (L1) C/A code receivers which allow instantaneous "precise" timing on the level of about one microsecond. These receivers may be used in the common view mode, where they observe the same satellite(s) (quasi-)simultaneously and the difference of observations referring to receiver pairs is analysed. In this mode the accuracy is limited by (a) the noise of C/A code, (b) differential ionospheric refraction, (c) the accuracy of station positions, and (d) the errors of the broadcast ephemerides.

The IGS/BIPM Project to Study Accurate Time and Frequency Comparisons, set up in December 1997 under the leadership of Drs. Jim Ray (US Naval Observatory USNO) and Claudine Thomas (Bureau International des Poids et Mesures BIPM), wants to fully exploit the potential of the GPS and the potential of the IGS network and analysis centers by (a) using the precise orbit and position information of the IGS and by (b) including geodetic-type GPS receivers at timing laboratories (which are connected to or driven by the best available time standards) into the IGS processing schemes.

Many technical problems (including precise measurements of cable delays, etc. of time transfer terminals) have to be addressed in this pilot project. It is also absolutely essential that the (geodetic type) receivers used for time transfer allow access to the receiver internal clock (which time-tags the observations); moreover the internal receiver clock must be identical for the phase and code observable.

It is expected that a highly operational and very accurate time transfer well below the nanosecond level (ideally a few ten picoseconds) will be achieved, and that frequency transfer will essentially only be limited

by the noise of the phase observable! It is also an important aspect that the "timing network" is properly incorporated into the IGS network.

Combining GPS and GLONASS

GLONASS, the Global NAvigation Satellite System, is the Russian counterpart of the GPS. It may be used in a similar way as the GPS for all purposes discussed so far and presumably with comparable accuracies. Essential GLONASS characteristics are:

- The full constellation nominally consists of 24 satellites (at present only 14 are "healthy").
- The satellites are regularly distributed in three orbital planes, separated by 120^o and inclined by 64.8^o with respect to the equatorial plane.
- The orbits are almost circular with semimajor axes of 25,510 km (giving rise to a revolution time of about $11^h\ 16^m$ (which means that the GLONASS orbits are not in deep 2:1 resonance with Earth rotation).
- Each satellite has its pre-assigned frequency in the range 1.603–1.616 GHz (L1) and 1.246–1.257 GHz (L2). The (pseudo random) code is identical for all satellites.
- GLONASS system time is essentially UTC (SU) which creates the problem of leap seconds — what analysts really like.

It is of particular interest that today we have geodetic combined GPS/GLONASS receivers, which track "all satellites in view" of both systems. The practical and scientific potential for combined analyses is remarkable:

- Navigation is much more reliable and robust.
- Thanks to the higher inclination of the GLONASS orbits the global coverage of a combined system is considerably improved.
- Sampling for atmosphere studies is much better.
- Resolving the initial integer ambiguities becomes easier if more satellites are observed simultaneously.

It is for these reasons that CSTG (Commission on International Coordination of Space Techniques), Commission B.2 of COSPAR and Commission VIII of IAG, and the IGS decided to organize IGEX-98, a three months International GLONASS Experiment towards the end of 1998. It is a global GLONASS tracking and analysis campaign which should give a good impression of the benefit of adding GLONASS to GPS and of the operational aspects of using the GLONASS. For more information we refer to Willis *et al.* (1998).

Spaceborne Applications of the GPS

It is becoming routine to deploy spaceborne GPS receivers on Low Earth Orbiters (LEOs). Such receivers may be used (a) for precise orbit determination (POD) and (b) for atmospheric sounding using the GPS occultation technique.

The first application is straight forward: code and phase observations from a GPS receiver (recorded usually by an antenna pointing in the radial direction away from the Earth) are used to reconstruct the trajectory of the LEO with an accuracy of a few centimeters. The TOPEX/POSEIDON Mission Fu *et al.* (1994) was

a kind of a "Rosetta Stone Mission" for POD using SLR and satellite microwave techniques (GPS and the French DORIS system). Fig. 23 (left) shows the TOPEX/POSEIDON spacecraft with the GPS antenna on the mast.

The IGS plays an important role for such applications: IGS orbits, and, depending on the actual processing technique used, precise GPS satellite and receiver clock estimates are used for the orbit determination of the LEO. For more information concerning POD using GPS we refer to Bertiger *et al.* (1994).

The GPS/MET mission was the proof of concept mission for atmosphere sounding using the GPS atmospheric occultation technique Yunck and Melbourne, (1996); Feng *et al.* (1994); Hajj *et al.* (1996). Many more missions will be based on the same technique. Fig. 23 (right) shows a picture (artist's view) of the German CHAMP mission (with a scheduled launch in 1999, see Reigber *et al.* (1998)) which will carry a spaceborne GPS receiver for occultation experiments.

The principle of the occultation technique is simple: the signal transmitted from a GPS satellite is tracked by the spaceborne GPS receiver (antenna pointing opposite to the direction of motion) until the signal is completely blocked by the Earth. As the signal cuts through the refractive atmosphere, the induced change of the phase delay may be measured. This delay, in turn, is associated with profiles of atmospheric density, pressure, temperature, or, in the ionosphere, electron density. The technique is illustrated by Fig. 24 (from (Yunck and Melbourne, 1996)). Depending somewhat on the orbit characteristics of the LEO the same technique (using the same occultations) may also be used for ionosphere monitoring by analyzing the two carrier phases.

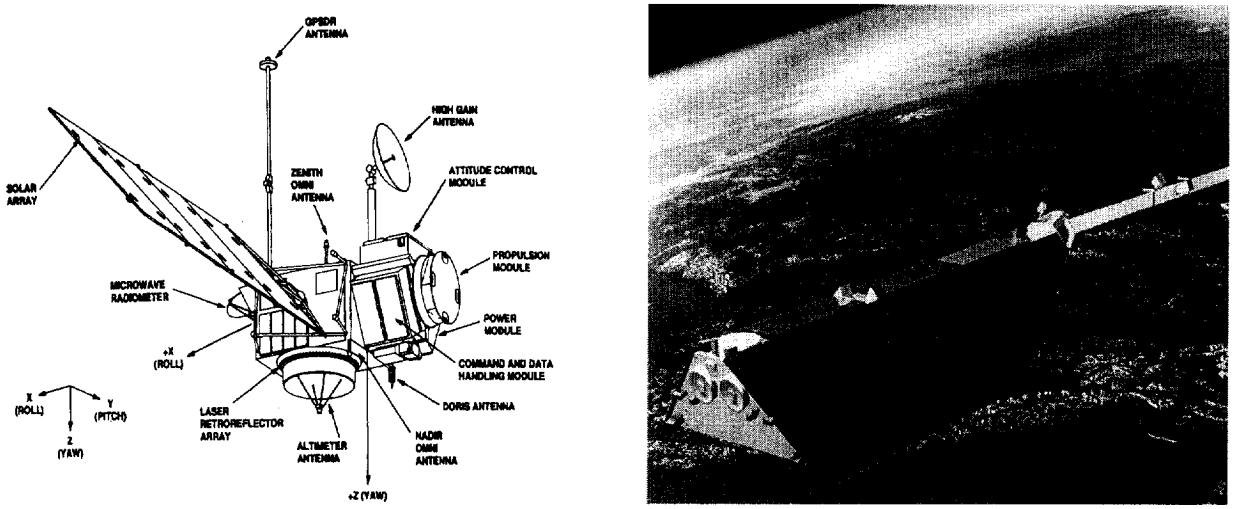

Fig. 23. TOPEX/POSEIDON Spacecraft, CHAMP Spacecraft

At first sight one might think that such occultations are rather rare events. One can easily verify, however, that up to 500 profiles per day may be recovered by only one LEO. A system of "cheap" micro-satellites might provide a truly complete series of tomograms of the Earth's atmosphere. Such techniques have the potential to revolutionize atmosphere science! For more information concerning spaceborne applications of the GPS we refer to Yunck and Melbourne (1996).

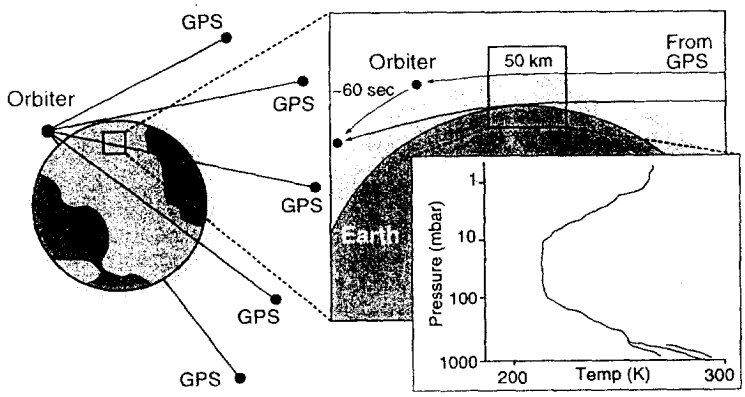

Fig. 24. The GPS Occultation Technique (from Yunck and Melbourne, 1996)

THE IGS AS AN INTERDISCIPLINARY SERVICE: SUMMARY AND CONCLUSIONS

We have shown in this overview that the IGS with its network, its analysis centers, and its working groups contributes significantly to the establishment of the terrestrial reference frame, to monitoring Earth Rotation (with high accuracy and with a high time resolution), to ionosphere monitoring by establishing global ionosphere maps and associated products, and to troposphere monitoring by combining and making available its troposphere-related products.

The IGS concept proved to be very powerful in the past. The IGS is getting ready right now to play a significant role for spaceborne applications of the GPS. It will be interesting to see how the IGS will meet the challenges of the future — in particular in view of spaceborne applications. It will be more difficult because the community interested in these new developments is more heterogeneous. Much will depend on the willingness of the IGS participants to continue working together in the future, and to be open to address new topics with the same enthusiasm. The authors of this overview have no doubt that this will be the case.

REFERENCES

Barnes, R.T.H., R. Hide, A.A. White and A. Wilson, Atmospheric angular momentum fluctuations, length-of-day changes and polar motion, in *Proceedings of Royal Society London, A*, Vol. 387, pp. 31–73, (1983).

Bauersima,I. NAVSTAR/Global Positioning System (GPS), (I), in *Mitteilungen der Satellitenbeobachtungsstation Zimmerwald, No. 7*, Druckerei der Universität Bern (1983).

Bertiger *et al.*, GPS Precise Tracking of Topex/Poseidon: results and implications, in Journal of Geophysical Research, Vol. 99, No. C12, pp. 24449–24464, (December 1994).

Beutler, G., I.I. Mueller, R.E. Neilan, The International GPS Service for Geodynamics (IGS): Development and Start of Official Service on January 1, 1994, in *Bulletin Géodésique, Vol. 68, 1*, pp. 39–70 (1994).

Beutler, G., J. Kouba, T. Springer, Combining the Orbits of IGS Processing Centers, in *Bulletin Géodésique*, Vol. 69, No. 4, pp. 200–222, (1995).

Beutler, G., I.I. Mueller, R.E. Neilan, The International GPS Service for Geodynamics (IGS): The Story, in *International Association of Geodesy Symposium, No. 115, GPS Trends in Precise Terrestrial, Airborne, and Spaceborne Applications.* pp. 3–13, Springer-Verlag, ISBN 3-540-60872-6 (1996).

Bevis, M., S. Businger, T.A. Herring, C. Rocken, R.A. Anthes, R.H. Ware, GPS Meteorology: Remote Sensing of Atmospheric Water Vapor using the Global Positioning System, in *Journal of Geophysical Research*, Vol. 97, pp. 75–94 (1992).

Boucher, C., Z. Altamimi, International Terrestrial Reference Frame, in *GPS World*, Vol. 7, No. 9, pp. 71–74

(September 1996).

Feng, D., B. Herman, M. Exner, W. Schreiner, R. McCloskey, D. Hunt, Preliminary Results from the GPS/MET Atmospheric Remote Sensing Experiment, in *International Association of Geodesy Symposium, No. 115, GPS Trends in Precise Terrestrial, Airborne, and Spaceborne Applications.* pp. 139–143, Springer-Verlag, ISBN 3-540-60872-6 (1996).

Feltens, J. and S. Schaer, IGS Products for the Ionosphere, in *Proceedings of the 1998 IGS Analysis Center Workshop* Darmstadt, Germany, (1998).

Fu, L.-L., E.J. Christensen, Ch.A. Yamarone, M. Lefebvre, Y. Ménard, M. Dorrer and Ph. Escudier, TOPEX/POSEIDON Mission Overview, in Journal of Geophysical Research, Vol. 99, No. C12, pp. 24369–24381, (December 1994).

Hajj, G.A., E.R. Kursinski, W.I. Bertiger, S.S. Leroy, T.K. Meehan, L.J. Romans, and J.T. Schofield, Initial Results of GPS-LEO Occultation Measurements of Earth's Atmosphere Obtained with the GPS-MET Experiment, in *International Association of Geodesy Symposium, No. 115, GPS Trends in Precise Terrestrial, Airborne, and Spaceborne Applications.* pp. 144–153, Springer-Verlag, ISBN 3-540-60872-6 (1996).

Manucci, A.J., B.D. Wilson and D.-N. Yuan, Monitoring Ionospheric Electron Content Using the GPS Global Network and TOPEX/POSEIDON Altimeter Data, in *Proceedings of the Beacon Satellite Symposium*, Aberystwyth, Wales, (1994).

McCarthy, D.D., IERS Conventions (1996), in *IERS Technical Notes No. 21*, Observatoire de Paris (1996).

Mueller, I.I., Planning an International Service Using the Global Positioning System (GPS) for Geodynamic Applications, in *IAG Symposium 109: Permanent Satellite Tracking Networks for Geodesy and Geodynamics*, Mader G. ed., pp. 1–22, Springer-Verlag, (1992).

Neilan, R.E., J.F. Zumberge, G. Beutler, J. Kouba, The International GPS Service: A Global Resource for GPS Applications and Research, in *Institute of Navigation, ION GPS-97, Proceedings*, pp. 883–889 (1997).

Neilan, R.E., IGS Colleague Directory, IGS Central Bureau, Jet Propulsion Laboratory, Pasadena (January, 1998).

Ray, R.D., D.J. Steinberg, B.F. Chao, and D.E. Cartwright, Diurnal and Semidiurnal Variations in the Earth's Rotation Rate Induced by Oceanic Tides, in *Science*, Vol. 264, pp. 830–832 (1994).

Reigber, Ch., H. Luehr, P. Schwintzer, Status of the Champ Geopotential Mission, in *Proceedings of the IAG Section II Symposium*, Munich, in preparation, (October 1998).

Rothacher, M., G. Beutler, T.A. Herring, R. Weber, Estimation of Nutation using the Global Positioning System, in Journal of Geophysical Research (accepted for publication, 1998a).

Rothacher, M., Recent Contributions of GPS to Earth Rotation and Reference Frames, in Habilitationsschrift, philosophisch-naturwissenschaftliche Fakultät der Universität Bern, Printing Office, University of Bern (1998b).

Salstein, D.A., IERS Sub-bureau for Atmospheric Angular Momentum Report, in *1996 IERS Annual Report*, pp. I-57–I-66, Observatoire de Paris (1997).

Schaer, S., G. Beutler and M. Rothacher, Mapping and Predicting the Ionosphere, in *Proceedings of the 1998 IGS Analysis Center Workshop*, Darmstadt, Germany, (1998a).

Schaer, S. and W. Gurtner and J. Feltens, IONEX: The IONosphere Map EXchange Format Version 1, February 25, 1998, in *Proceedings of the 1998 IGS Analysis Center Workshop*, Darmstadt, Germany (1998b).

Spilker, J.J., GPS Signal Structure and Performance Characteristics, in *Navigation, Journal of The Institute of Navigation (U.S.)*, Vol. 25, pp. 121–146 (1980).

Willis, P., G. Beutler, W. Gurtner, G. Hein, R.E. Neilan, C. Noll, J. Slater, IGEX: International GLONASS Experiment — Scientific Objectives and Preparation, in *this Volume* (1998).

Yunck, T.P. and W.G. Melbourne, Spaceborne GPS for Earth Science, in *International Association of Geodesy Symposium, No. 115, GPS Trends in Precise Terrestrial, Airborne, and Spaceborne Applications.* pp. 113–122, Springer-Verlag, ISBN 3-540-60872-6 (1996).

Zumberge, J.F., D.E. Fulton, R.E. Neilan, *International GPS Service for Geodynamics 1996 Annual Report*, IGS Central Bureau, Jet Propulsion Laboratory (1997).